Forest Ecology and Management 524 (2022) 120525

Contents lists available at ScienceDirect

Forest Ecology and Management

journal homepage: www.elsevier.com/locate/foreco

Modeling potential site productivity for *Austrocedrus chilensis* trees in northern Patagonia (Argentina)

Facundo J. Oddi [a,b,*], Cecilia Casas [c,d], Matías G. Goldenberg [a,b], Juan P. Langlois [c], Jennifer B. Landesmann [e], Juan H. Gowda [e], Thomas Kitzberger [e], Lucas A. Garibaldi [a,b]

[a] Universidad Nacional de Río Negro, Instituto de Investigaciones en Recursos Naturales, Agroecología y Desarrollo Rural, Río Negro, Argentina
[b] Consejo Nacional de investigaciones Científicas y Técnicas, Instituto de Investigaciones en Recursos Naturales, Agroecología y Desarrollo Rural, Río Negro, Argentina
[c] Universidad de Buenos Aires, Facultad de Agronomía, Departamento de Recursos Naturales y Ambiente, Cátedra de Edafología, Av. San Martín 4453, C1417DSE Buenos Aires, Argentina
[d] IFEVA, Universidad de Buenos Aires, CONICET, Facultad de Agronomía, Av. San Martín 4453, C1417DSE Buenos Aires, Argentina
[e] CONICET, INIBIOMA-Universidad Nacional del Comahue, Quintral 1250, 8400 Bariloche, Río Negro, Argentina

ARTICLE INFO

Keywords:
Site quality
Native forestry
'ciprés de la cordillera'
Climate
Soil properties
Multi-model inference

ABSTRACT

Sustainable management of native species is essential in regions where forest is continually decreasing, such as South America. A first step for sustainable management is to develop models of productivity and site quality, which are usually related to the height of dominant trees. The aim of this study was to model the height (*h*) of dominant trees of southern South American conifer *Austrocedrus chilensis* based on climate, topography and soil predictors, and tree age using a mixed-effect modeling approach under a multi-model inference framework. Tree data (*h* and age) were collected in 43 plots placed throughout the natural distribution range of *A. chilensis* in northern Patagonia (Argentina). Soil characterization was carried out in 32 out of 43 plots. Our results indicate that dominant trees are taller in cooler and wetter sites with more soil carbon and lower soil acidity. The model predicted *h* with ≈3 m (19 %) error and explained about 85 % of variability in *h* (conditional $R^2 = 0.84$). When considering only climate variables, the explained variance was reduced by 7 % although the loss of predictive capability was not substantial (3.1 m prediction error). This study provides the first regional statistical model predicting productivity indicators in *A. chilensis*. With this model, site quality can be classified just using a few climatic variables available from satellite-based geospatial information and then improved by including edaphic information (soil carbon, pH). The model could have usefulness beyond forestry, for example to foresee climate change effects on ecosystem services associated to forest productivity.

1. Introduction

Forests play a key role in mitigating climate change and providing ecosystem services for human well-being (FAO and UNEP, 2020). Forest capacity to continue providing ecosystem services depends on sustainable management practices –both under current and forecasted climate scenarios. Traditionally, however, landowners prioritize timber production over other forest services such as carbon sequestration, water provision and biodiversity conservation. Given the exponential increase in human population, thus increasing demand on goods and services from forests, the paradigm of sustainable forestry is getting remarkable attention for forest policy and management (O'Hara, 2016). Sustainable forest of native species may offer an appealing productive alternative (Donoso and Soto, 2010; Promis, 2020) and congruent with the conservation of ecosystem services, the restriction in the use of exotic species, and the production of high-quality timber (Pro Silva, 2012). However, its adoption by landowners and government agencies is prevented when the base knowledge to support the management of native species is not available (Davis et al., 2012).

Knowledge of inherent site productivity is essential for developing sustainable forestry (Bontemps and Bouriaud, 2014). Productivity depends on complex biotic, climatic, topographic, and edaphic interactions, which are summarized in the concept of 'site' (Skovsgaard and Vanclay, 2013). The quality of a site is species-specific (each species has an optimal environment) and defines its potential for plant biomass production (Assmann, 1970); when environmental conditions are more

* Corresponding author.
E-mail address: foddi@unrn.edu.are (F.J. Oddi).

https://doi.org/10.1016/j.foreco.2022.120525
Received 26 May 2022; Received in revised form 30 August 2022; Accepted 5 September 2022
Available online 13 September 2022

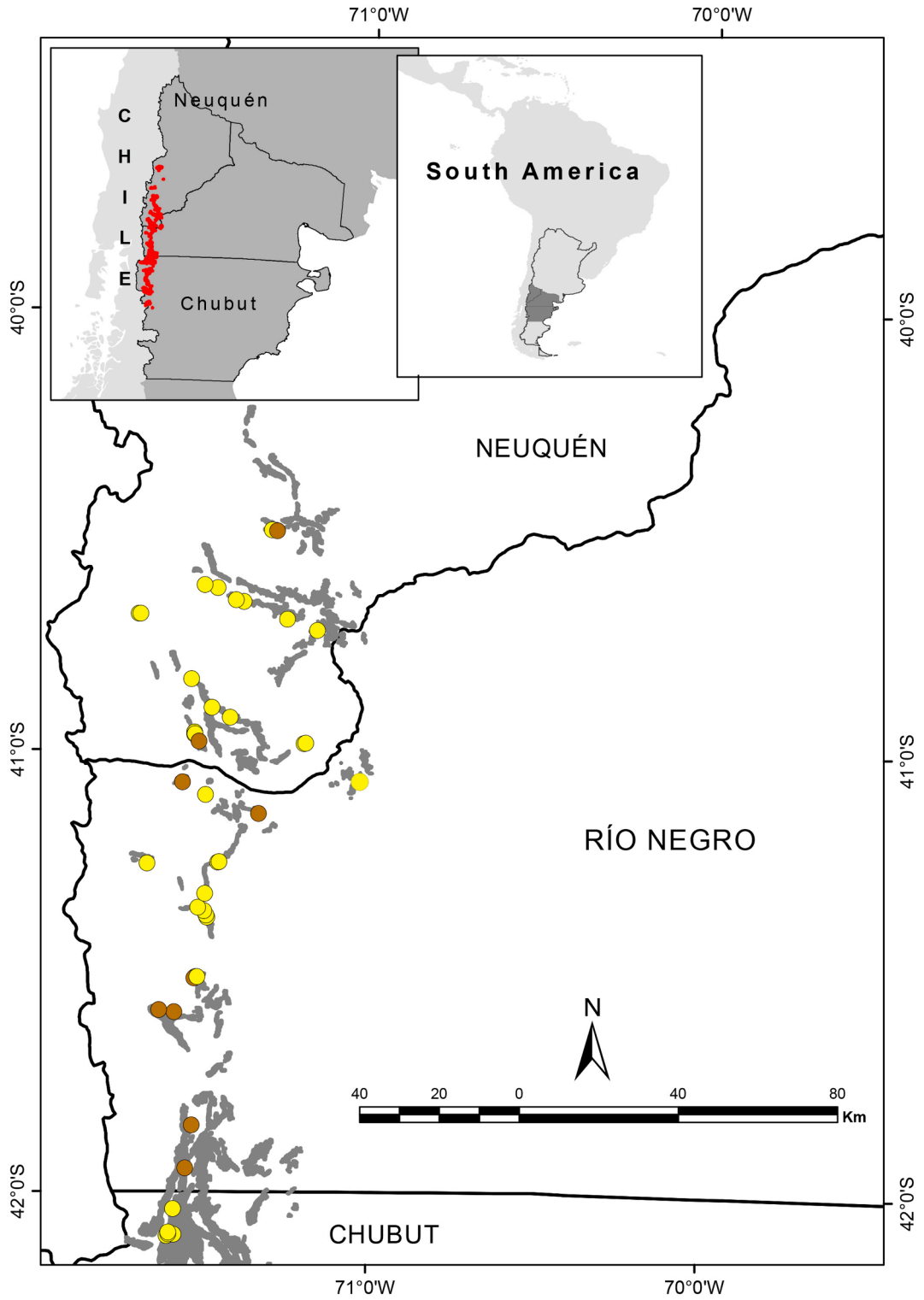

Fig. 1. Study area and sampling plots. Dots show sampling plots. Brown and yellow filling indicate plots where climate-topography or climate-topography and soil variables were measured, respectively. Top left inserted map shows the natural distribution of *Austrocedrus chilensis* (Argentina).

favorable for a given species, that is, when site quality improves, productivity increases –according to Skovsgaard and Vanclay (2008) site productivity is a quantitative estimate of site quality. Classifying and mapping sites according to their quality (that is, categorizing site productivity in quality levels) contributes to developing forest policy strategies at regional and national scales (Bontemps and Bouriaud, 2014).

Forest productivity is often difficult to define and measure, thus proxies are usually used (Burkart and Tomé, 2012). Sites are frequently classified by top height at a reference age (referred as base age), which is a widely used site quality index. This index is based on the idea that forest productivity correlates with the height of dominant trees (top height) (Skovsgaard and Vanclay, 2008). However, in sites where the species to be afforested is not present, environmental variables –including climate, topography and soil properties– must be used (Weiskittel et al., 2011). Modeling vegetation-based indicators of site productivity (e.g., top height) according to site physical characteristics

allow assessing quality of sites for forestry development (Aertsen et al., 2010).

Austrocedrus chilensis (D.Don) Pic. Serm. et Bizzarri is a tree species native to northern Andean Patagonia with high economical value (Goya et al., 2004). Its wood is weather-resistant and one of the most traded in the region (Letourneau et al., 2005); traded-wood typically comes from dead trees that suffered from "mal del ciprés", a *Phytophthora*-caused disease (Loguercio et al., 2005). *A. chilensis* forests also provide several non-timber resources (Ladio, 2005). Despite the economic value of this species (Goldenberg et al., 2018), its management is still incipient (Loguercio et al., 2018). Usually forestry is combined with livestock raising, which harms both natural recruitment of saplings and wood quality (Loguercio et al., 2005). In healthy stands, simple management schemes based on site quality are suggested for promoting tree growth and improving bole characteristics (Loguercio et al., 2018). Regarding environmental conditions affecting productivity, previous studies have described that the growth of *A. chilensis* shows a regional pattern increasing with precipitation, and that it also responds favourably to wetter local conditions (Dezzotti and Sancholuz, 1991 Veblen et al., 2005). Locally, other studies (Marcotti et al., 2021; Mundo et al., 2010) have found that *A. chilensis* growth is strongly affected by water deficit, mediated by temperature and soil water content. Although water availability has been established as one of the main drivers of *A. chilensis* growth, site productivity models have yet to be developed for this species. The lack of productivity models become ever more relevant when considering that the current Argentinian regulatory framework promotes native species plantations thus commercial plantations of *A. chilensis* are expected to be established in the near future (Aparicio and Pastorino, 2020), even outside its natural range (Oddi et al., 2021).

The aim of our study was to model the height of *A. chilensis* dominant trees from climate, topography and soil properties in northern Patagonia. Considering that *A. chilensis* stand height is an indicator of its site quality (Dezzotti and Sancholuz, 1991), we expect that (once discounting the effect of age) top height to increase as environmental conditions favor soil moisture availability. From an applied perspective, we expect that our modeling approach of site productivity of *A. chilensis* will contribute with regional classification of site quality, serving as a tool for forest planning.

2. Materials and methods

2.1. The species

The species *Austrocedrus chilensis* (known as 'ciprés de la cordillera' or 'Chilean cedar') is a long-lived (can live more than 500 years) slow-growing perennial conifer (Cupressaceae) native to Argentina and Chile (Aparicio and Pastorino, 2020). Although it grows on both sides of the southern Andes, ~75 percent of their natural distribution occurs on the eastern side, in Argentina (Serra et al., 2015). There, the latitudinal range of the distribution of *A. chilensis* extends from 37°07′S to 43°44′S covering about 260.000 ha (Pastorino et al., 2006; Pastorino et al. 2015). Longitudinally, it occupies a narrow strip of 60–80 km width. This species thrives under a wide range of environments and individuals are highly variable in shape and size (Veblen et al., 2005): conical-shaped taller than 35 m trees are observed under wetter conditions (Aparicio and Pastorino, 2020) while multi-stemmed 3 m tall individuals are frequent towards dry conditions (Castor et al., 1996 and references therein). The eastern marginal populations are the most genetically diverse although genetic variability has a rather latitudinal spatial arrangement (Pastorino et al. 2015). The origin, dynamics and age structures of *A. chilensis* stands are related to disturbances (mainly fire) and vary with site conditions (Dezzotti and Sancholuz, 1991; Serra et al., 2015; Veblen et al., 2005, 1995; Veblen and Lorenz, 1987; Villalba and Veblen, 1997).

2.2. Study area

The region of northern Patagonia includes the Argentine provinces of Neuquén, Río Negro, and Chubut (Fig. 1). Geomorphologic processes formed the southern Andes and shaped environmentally heterogeneous landscapes (Matteucci, 2012). Westerlies carry humid air masses from the Pacific Ocean that are lifted and cooled as they cross the north–south-oriented Andes Mountains, generating cyclonic precipitations (Paruelo et al., 1998). Most precipitation falls on the western slopes of the Andes in Chile and, eastward, precipitation decreases from more than 2000 mm yr^{-1} to less than 500 mm yr^{-1} in ~ 100 km (Bianchi et al., 2016). Forest types change according to this steep west-to-east precipitation gradient, topography and edaphic characteristics (Dezzotti and Sancholuz, 1991; La Manna, 2005; Veblen and Lorenz, 1987). Through the gradient, mixed forests, pure and dense forests, pure and sparse forests, and marginal woodlands are observed (Dezzotti and Sancholuz, 1991; Serra et al., 2015). Rainfalls occur concentrated in the winter months (Paruelo et al., 1998) and combined with dry summers result in a Mediterranean type-climate (Kottek et al., 2006). The Andisol soil order dominates the soils on the wetter portion of the gradient, whereas Mollisols and Alfisols characterize the soils eastward (Mazzarino et al., 1998).

2.3. Data collection

A stratified sampling was applied on the Argentine side of the *A. chilensis* distribution and 46 plots were selected (Fig. 1). To encompass the widest possible range of environmental conditions, the stratification was based on maps of annual precipitation (Cordon et al., 1993) and vegetation (Gowda et al., 2010), which were superimposed on a digital elevation model (ASTER GDEM Validation Team, 2011). The selected plots (Fig. 1) covered from Lake Filo Hua Hum (40°30′7.02″S, 71°17′5.94″W, Neuquén) at north to Lago Puelo (42° 6′1.26″S, 71°36′22.02″W, Chubut) at south, mostly covering the western edge of Patagonia region (Argentina), where pure and mixed cypress forests occur. In Argentina, most of *A. chilensis* forests are not managed, eliminating a potential confounding factor for site productivity evaluation (Skovsgaard and Vanclay, 2008).

In the spring of 2012, circular plots were defined in the field recording with GPS the geographical coordinates of its centre. Stands dominated by *A. chilensis* with uniform spatial distribution and approximately uniform diameter were selected. Plots included at least 10 adult individuals (variable-radius plots) and were placed in sites where trees were free of suppression/liberation signals (for instance, evidence of fire —charred bark, scar at tree base etc.—, windthrow —tree fall—, or pest). In each plot, diameter at breast height of all trees of diameter > 8 cm (DBH) was measured with a dendrometric tape. Trees were counted and *A. chilensis* density was determined. The height of the three largest DBH individuals (assumed as dominant trees) was measured (Häglof HEC-MD electronic clinometer) and their wood cores extracted at 0.4 m height for age determination by counting the rings. The sampled cores (138 = 46 plots × 3 dominant trees per plot) were prepared in holders, which allowed their surfaces to be cut and the broken cores to be assembled. When core centres were not reached (seven samples), age was estimated as proposed by Duncan (1989); the number of missing rings was calculated as the missing radius divided by the average width of the last three rings. This formula is not valid for rings with irregular shapes so that visual estimation was used when necessary. Finally, age was estimated for 93 out of 138 cores as 45 of these could not be properly prepared for reading and were discarded from analysis (three plots were not considered because all their tree cores were discarded).

2.4. Climatic, topography and soil variables

The climatic variables assessed were average annual precipitation

Table 1
Sampling variables recorded at different levels, type of indicator that they represent, and punctual estimate (s) and 95% confidence interval (CI) of the Spearman's correlation coefficient of height to all the quantitative variables.

Variable	Level	Variable	Unit	Sampling summary statistics					Spearman correlation	
				Mean	Min.	Max.	Std. deviation	Coef. Var.	s_p	95 % CI
stand structure	*tree*	*height (response)*	*meter*	17.6	8.0	36.2	5.4	0.31	–	–
		age	*year*	93.8	44	246	50.4	0.54	0.60	0.44; 0.72
	plot	*A. chilensis density*	*tree ha^{-1}*	1887	97	5305	1313.6	0.70	0.01	−0.20; 0.22
soil	*plot*	*soil organic matter (SOM)*	*%*	17.3	3.7	36.2	7.0	0.40	0.26	0.02; 0.49
		particulate organic matter (POM)	*%*	9.9	1.0	30.9	5.4	0.54	0.07	−0.17; 0.31
		Mineral-associated organic matter (MAOM)	*%*	12.4	2.2	26.4	5.2	0.42	0.26	0.02; 0.44
		POM:MAOM ratio		2.25	0.18	9.6	1.5	0.67	0.16	−0.08; 0.39
		phosphorus content	*p.p.m.*	10.8	3.0	29.6	5.7	0.53	0.30	0.06; 0.51
		nitrogen content	*%*	0.3	0.1	0.7	0.1	0.33	0.21	−0.04; 0.42
		electrical conductivity	*dS m^{-1}*	0.16	0.03	0.44	0.08	0.50	0.41	0.17; 0.62
		pH		6.2	5.3	7.2	0.45	0.07	0.08	−0.12; 0.26
		pH NaF		8.7	7.2	10.6	1.2	0.14	−0.03	−0.24; 0.19
		sand content	*%*	63.2	37.5	83.9	11.1	0.18	−0.28	−0.48; −0.07
		silt content	*%*	20.7	1.5	46.7	12.1	0.58	0.10	−0.14; 0.33
		clay content	*%*	14.9	19.2	45.3	10.9	0.73	0.26	0.03; 0.44
topography	*plot*	*elevation*	*m.a.s.l.*	792.3	212.0	991.0	197.9	0.25	−0.30	−0.48; −0.10
		slope	*%*	12.4	2.0	39.0	9.5	0.77	−0.25	−0.45; −0.02
		northing	–	0.59	0	1	0.29	0.49	−0.28	−0.47; −0.06
		easting	–	0.44	0	1	0.28	0.64	−0.15	−0.34; 0.07
climate	*plot*	*annual precipitation*	*mm yr.$^{-1}$*	1455	500	2333	378.9	0.26	0.13	−0.08; 0.33
		average summer temperature	*°C*	14.0	12.3	18.6	1.2	0.08	−0.31	−0.49; −0.12

and average summer temperature. Average annual precipitation (thereafter *annual precipitation*) data were obtained from interpolating the isohyets published in (Cordon et al., 1993) with the IDRISI software (interpolation module contour –INTERCONN; Eastman, 2009). We extracted average monthly data (March 2000 - September 2012), in °C, from "Land surface temperature and emissivity MOD11A2″ (ORNL DAAC, 2011). This MODIS product provided temperature data with an approximate frequency of two-data every 8 days for a 1-km^2 area. Average summer temperature (thereafter *summer temperature*) was calculated as the average 2000–2012 of the average (Dec - Feb) months. By using MODIS series (contemporary data), it is assumed that the spatial trends of temperature have not changed since stand establishment (i.e., the warmest/coolest sites today were also the warmest/coolest sites hundred years ago).

Topography was characterized according to slope (%), elevation (m. a.s.l.) and aspect. Slope was measured in the field by using an electronic inclinometer (Häglof HEC-MD), whereas elevation and aspect were derived from the earth's surface "ASTER Global Digital Elevation Model" (ASTER GDEM validation team 2011). Aspect was expressed on a 360° scale (north = 0°, south = 180°, east = 90°, west = 270°) and cosine-transformed into *northing*, a linear variable expressed in radians where 1 indicates north, −1 indicates south, and 0 is equal to east and west.

Composite soil samples (n = 3) were taken at 0–20 cm depth in 32 out of the 43 sampling plots with available cores. Samples were randomly selected within plots avoiding points near the border and thick roots in order to represent the average conditions of the soil among *A. chilensis* trees. The soil samples were air dried and sieved (2 mm). The percentage of soil organic matter (SOM) and their main fractions: particulate and mineral associated organic matter (POM and MAOM, respectively) were determined by sieving (53 μm) (Cambardella and Elliott, 1992) and ignition (550 °C for 5 h) (Mirsky et al., 2008). Briefly, 25 g of soil were stirred for 30 min in a dispersant solution of 5 % sodium hexametaphosphate [5 g L (NaPO3) 6], and then passed through a 53 μm sieve. The material that remained on the sieve was used to determine the POM and that which passed through the sieve, the MAOM. Both fractions were collected in beakers and placed in an oven at 50 °C, until the moisture content was eliminated. The resulting dry material was then collected and placed in a muffle at 550 °C for 8 h. The POM and MAOM was obtained by subtracting the weight of the sample after and before ignition. SOM was calculated as POM plus MAOM and the corresponding percentages were calculated as those fractions divided by sample dry weight × 100. In addition, soil samples material was used to determine the pH (1:2.5 in water), electrical conductivity [c.e. (dSm^{-1}) saturated paste], nitrogen content (N, Kjeldahl) (Bremner, 1960), phosphorus content (P, Olsen) and the granulometric composition. The granulometric composition of the soil samples was determined using the Robinson pipette method (Pansu and Gautheyrou, 2006).

2.5. Data analysis

2.5.1. Data handling and modeling approach

Individual relationships between top height and the remaining sampled variables were explored graphically, and the Spearman correlation (s_p) was estimated (Table 1). The use of top height as an indicator of productivity assumes that (top height) is not affected by stand density (Skovsgaard and Vanclay, 2008). No graphical association was observed between height and density (expressed either in absolute terms –trees per hectare– or as a Reineke index) and this conclusion was supported by the Spearman correlation, which was near to zero ($\widehat{s}_p$ = 0.01; Table 1). Environmental predictors were centered at the mean to reduce collinearity, which was evaluated by calculating pairwise Pearson correlations (Table A1) and the variance inflation factor (VIF). In the case of the age, for more generality it was centered at 90 years (sampling mean = 93.8 years). This age is close to the cutting cycle of the species suggested in the literature (Aparicio and Pastorino, 2020; Goya et al., 2004). Top height was modeled by fitting a linear mixed-effects model with climate, topographic and soil predictors, plus age, which accounted for the lack of independence imposed by the hierarchical sampling design, i.e., trees nested within plots, plots nested within localities. To deal with the inherently nonlinear relationship between age and height, age was base 2 log-transformed; log transformation over x accounts for a decreasing-with-age growth rate and base 2 simplifies the meaning of the parameter (top height increment when doubling age). To avoid negative numbers (as a result of centering age at 90) that prevent using logarithms, the variable finally included in the model was log_2(age) – log_2(90).

2.5.2. Multi-model inference

The initial fixed components of the model [Eq. (A.1) Appendices] were: *age* (at the tree-level), *annual precipitation* (*Pp*), *summer temperature* (*Ts*), *elevation* (*elev*), *slope*, *northing* (*expN*), *MAOM fraction* (*maom*), *POM:MAOM ratio* (*pmr*), *soil nitrogen content* (*N*), *soil phosphorus content*

(*P*), *sand content (sand)*, *pH*, and e*lectrical conductivity* (*ec*), all as predictors at the plot-level (Table 1). Selected two-way interactions based on ecological relevance were also included (*Pp:Ts*, *Pp:expN*, *Ts:maom*, *Pp:maom*, *Pp:sand*). The model was fitted by restricted maximum likelihood and included random effects for the intercept at the plot level (the fit was not improved by including random effects at the locality level). We performed a graphical inspection of the models to evaluate their adequacy by plotting: *i*) standardized residuals against fitted values and the predictive variables, *ii*) a quantile–quantile distribution of standardized residuals and, *iii*) a variogram of standardized residuals on latitude and longitude to evaluate spatial correlation (Zuur et al., 2009).

Fixed effects were evaluated by multi-model inference of the complete model re-estimated by maximum likelihood. All the possible combinations of fixed effects were fitted (in total 35,072 models including the null model, i.e., the model with the same random structure but no fixed effects) using 32 plots and 69 trees. The analysis was performed with the 'Akaike Information Criterion' with correction for small sample sizes (AICc) as a parsimony indicator (Burnham et al., 2011). For each model (*m*), the difference in AICc (Δ_m) with respect to the AICc of the best-ranked model (i.e., that with minimum AICc) was computed as well as its 'Akaike weights' (w_m), that is, its relative likelihood normalized over that of all models of the set. Those models with $\Delta_m < 2$ were considered to have similar evidence support and were ranked as the set of the best models. The relative importance (*ri*) of each fixed-effect predictor (*p*) was evaluated by summing w_m over all models. Predictors with $ri > 0.6$ were considered as importantly related to *A. chilensis* top height (Cinar et al., 2021).

2.5.3. Goodness-of-fit and predictive capability

Both the marginal and conditional R^2 [*sensu* Nakagawa and Schielzeth (2013)] were used as goodness-of-fit metrics (how well the models fit to data). These marginal and conditional R^2 represent the proportion of variance explained by the fixed effects, and by the fixed and random effects combined (i.e., the entire model), respectively (Nakagawa and Schielzeth, 2013). To evaluate the predictive capability (how well the models predict new data), cross-validation procedures were applied (Yang and Huang, 2014). The dataset used to fit the models (32 plots, 69 trees) was partitioned according to plots into five disjoint subsets (≈20 % of the data per subset). The models were repeatedly trained on four subsets and prediction metrics in the remaining subset were obtained, in such a way that each subset was used as a test set once (*K*-fold cross-validation). Then, each metric was averaged over the five iterations. The metrics used to quantify the predictive capability were the mean absolute error [*mae*; Eq. (A.2) Appendices] and the mean absolute percent error [*mape*; Eq. (A.2) Appendices] (Yang and Huang, 2014).

Regional maps of site quality require predictive models of productivity based on spatial layers at that scale, and climate/topography information is available from remotely sensed data. Although remarkable progress in mapping edaphic characteristics at global scale has been made recently (Hengl et al., 2017; Poggio et al., 2021), they entail time-consuming field and lab procedures that require high-level technical expertise. Therefore, it would be particularly useful to evaluate models that include only climate and/or topographic variables. Hence, the performance of the models that included only climate and/or topographic variables was compared with that of the best-ranked model. In addition, those plots where soil variables were not collected (11 plots, 24 trees) were used as an independent validation dataset to test the predictive capability (*mae* and *mape*) of the best climate/topography models. Finally, a climate/topography model was selected to predict the height of dominant trees over the region at an age base of 90 years.

All the analyses were performed with R 4.0.3 (R Core Team, 2020). The lme() function of the nlme package (Pinheiro et al., 2020) was used to fit the models. The dredge(), subset.model.selection() and importance () functions of the MuMin package (Barton, 2020) were used in the multi-model analysis. The fold() function of the groupdata2 package (Olsen, 2021) and the cross_validate() function of the cvms package

Table 2
Best models as ranked by AICc (ΔAICc (Δ_m) < 2; AICc best-ranked model = 363.5). Each row represents one model and columns provide information about each model. Plus and minus signs indicate whether the estimates of the fixed-effects (columns) of each model were positive or negative, respectively. Shadow cells indicate that the fixed-effect (column) is not included in the model (row). Fixed-effects are informed as termed in Eq. (A.1). Two of the best-ranked climate/topography models (*ctm*) as ranked by AICc and the *null* model are also included. The relative importance (*ri*) of each predictor is informed in the last row.

Rank	Fixed-effects																		Δ_m
	Climate			Topography			Soil							Interactions					
	age	*Pp*	*Ts*	*elev*	*slope*	*expN*	*maom*	*pmr*	*N*	*P*	*sand*	*pH*	*ec*	*Pp:Ts*	*Pp:expN*	*Ts:maom*	*Pp:maom*	*Pp:sand*	
1	+		−				+					+							−
2	+		−				+												0.40
3	+	+	−				+					+							0.70
4	+	+					+				−	+						−	0.73
5	+	+	+				+					+							1.37
6	+	+	−				+				−	+						−	1.47
7	+	+					+			+	−	+						−	1.88
8	+		−				+	−				+							1.92
9	+		−	−			+					+							1.95
24 (ctm)	+		−																2.44
76 (ctm)	+	+	−											−					3.48
18,005 (null)																			20.63
ri	1.00	0.64	0.71	0.28	0.22	0.36	0.65	0.28	0.23	0.26	0.37	0.54	0.34	0.14	0.12	0.10	0.10	0.22	

Table 3
Estimated parameters (CI 95% in square brackets) for the best-ranked model (Table 2). Predictors include units and they are termed as in Eq. (A.1) Appendices. The estimated value for σ_{plot} is 2.78 and for σ is 2.12.

Predictor	Estimate [CI 95 %]
intercept (m)	17.642 [16.496, 18.788]
age (yr.)	4.586 [2.943, 6.230]
summer temperature (°C)	−1.303 [-2.099, −0.506]
maom (%)	0.254 [0.027, 0.480]
pH	2.274 [-0.413, 4.961]

(Olsen and Zachariae, 2021) were used for cross-validation procedures. Maps were created using QGIS version 3.10 (QGIS Development Team 2019).

3. Results

3.1. Model fitting and multi-model inference

The height of dominant trees of *A. chilensis* ranged from 8 m to 36 m, and the age from 44 to 246 years (Table 1). This variability was mainly explained by the *age* ($ri = 1$) of the individual trees followed by *summer temperature* ($ri = 0.71$), *annual precipitation* ($ri = 0.64$), and soil *MAOM* content ($ri = 0.64$) (Table 2). The best-ranked model (Table 3) predicted a top height of ≈17 m for *A. chilensis* trees of 90 years old (Fig. 2a) under average environmental conditions, and an increase by 4.6 m per one-unit increase in log_2 age (i.e., doubling age) in the sampled range from 40 to 250 years old. According to this model, top height decreased with *summer temperature* at a rate of 1.3 m per °C and increased 25 cm each percent increment in *MAOM*. *Annual precipitation*, the second most important environmental predictor, was not selected in the best-ranked model but was included in many of the best models (i.e., those with $\Delta_m < 2$; Table 2) and in all cases, the estimate was positive. Interestingly, more than half of these models also included a negative interaction between *annual precipitation* and soil *sand* concentration, suggesting that the positive relation of *annual precipitation* and top height decreased as the *sand* content increased. Soil *pH* also was included in the best-ranked model, as well as in the most of the best models (all of them indicating a positive relationship), although their relative importance was lower than 0.6 (Table 2). Our modeling approach, applied to the available data, suggests that the remaining environmental predictors were not importantly related with *A. chilensis* top height (Table 2).

When analysing models only with climate and/or topography (plus age) predictors, the best-ranked model only included *summer temperature*. The AICc of this model differed in less than 2.5 units with respect to that of the general best-ranked model (Table 2). The AICc of the conceptually relevant model including *summer temperature* interacting with *annual precipitation* increased ≈1 with respect to that of the previous model (Table 2), suggesting they have similar fit. This model improves the likelihood respect to that with only *summer temperature* (-175.5 vs −177.4), at the cost of greater complexity (5 fixed parameters vs 3 fixed parameters). These models ranked 24th and 76th, respectively, and largely reduced the AICc compared to that of the null model (Table 2).

3.2. Goodness-of-fit and predictive capability

Although there were differences between models with and without soil predictors in terms of variance explained, the predictive capacity did not substantially decrease when only climatic and/or topographic variables (plus age) were considered. The fixed factors of the best-ranked model explained 58 % of the total variability of *A. chilensis* top height, reaching 84 % when random effects were considered (marginal and conditional R^2, respectively; Table 4). On average, in this model the difference between the predicted and observed (*mae*) for the height of dominant trees was 3.07 m, or 18.8 % if the difference is expressed in

Table 4
Performance (goodness-of-fit and predictive capability) of the best-ranked model (overall fit) and that of best models only including climate and/or topography predictors (proposed for top height mapping; the two best-ranked climate/topography models ranked 24th and 76th overall, Table 2). Metrics of predictive capability (*mae*: mean error absolute; *mape*: mean absolute percent error) were assessed on the dataset used in the fit (*K*-fold cross-validation; $n = 69$) and an independent validation dataset in the case of climate/topography models was also used ($n = 24$). All models include *age* as a predictor (*Ts*: summer temperature; *maom*: MAOM fraction; *pH* = soil pH; *Pp*: annual precipitation).

		Overall (soil + climate + topography)	**Mapping (climate + topography)**	
		1st-ranked	24th-ranked	76th-ranked
Goodness-of-fit	fixed component	*Ts + maom + pH*	*Ts*	*Ts × Pp*
	R^2 marginal	0.581	0.458	0.514
	R^2 conditional	0.839	0.832	0.833
predictive capability *K*-fold cross-validation	*mae* (m)	3.07	3.18	3.12
	mape (%)	18.8	20.1	18.9
predictive capability independent validation dataset	*mae* (m)	–	3.86	3.43
	mape (%)	–	22.5	20.1

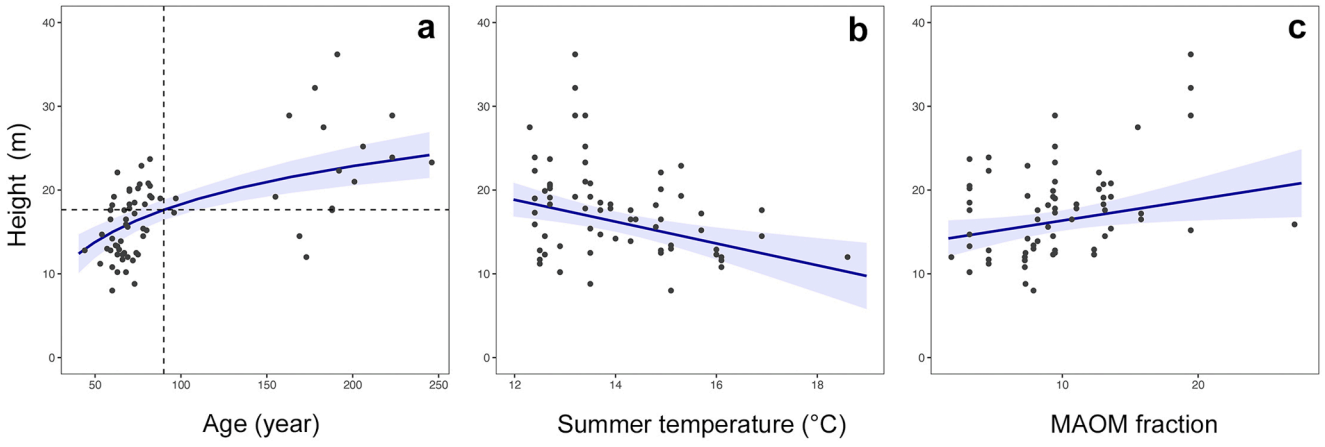

Fig. 2. *A. chilensis* top height predicted from the best-ranked model (Table 2). Top height predictions generated varying a) *age*, b) *summer temperature*, c) *MAOM* fraction, and holding the remaining predictors at the mean (dotted lines in the left-side plot highlight top height predicted at age 90).

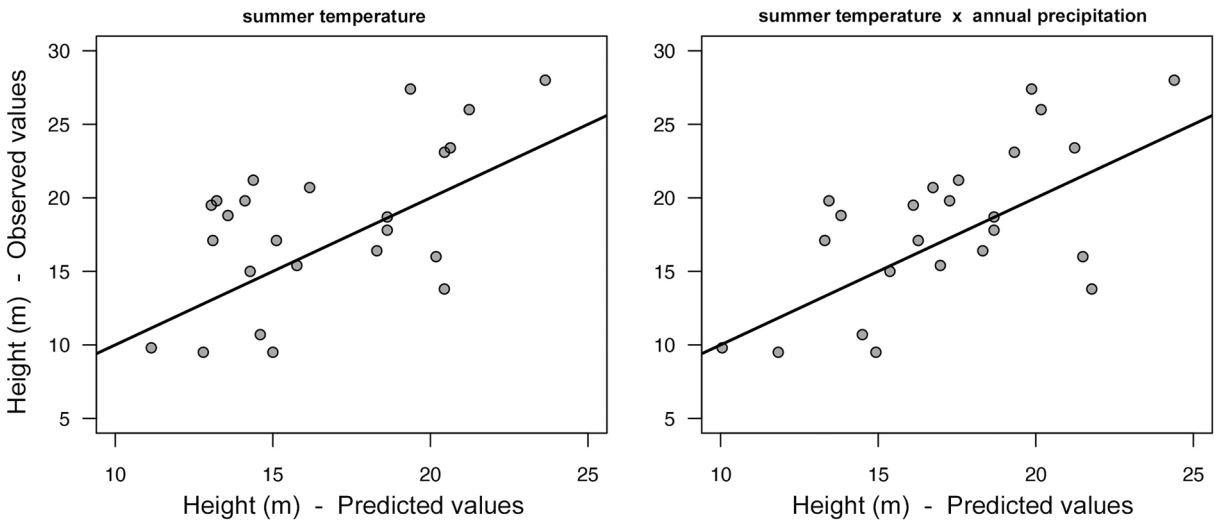

Fig. 3. Predictive capability of two best-ranked climate/topography models (proposed for top height mapping, Table 3) assessed using an independent validation dataset. The one-to-one line is included on each plot to observe the model prediction errors (i.e., observed heights –points– minus predicted heights –line–).

relative terms (*mape*).

The marginal and conditional R^2 of the best-ranked climate/topography model, i.e., the model with only *summer temperature* as environmental predictor, were 46 % and 83 %, respectively (Table 4). When including *summer temperature* interacting with *annual precipitation*, these R^2 were 51 % and 83 %, respectively (Table 4). This model predicted top height with an error of 3.12 m (*mape* = 18.9 %), whereas the best-ranked climate/topography model (only *summer temperature*) increased this error to 3.18 m (*mape* = 19.6 %) (Table 4). Nevertheless, when we validated these models using the independent dataset (Fig. 3), the prediction error of the simplest model was 3.46 m (*mape* = 20.1 %) and that of the interaction model was 3.86 m (*mape* = 22.5 %) (Table 4). Since the performance of the climate/topography models (fit and predictive capability, the latter on the validation dataset), we selected the simplest one (*summer temperature*) to illustrate as top height could be predicted at age 90 over the study area (Fig. 4).

4. Discussion

A. chilensis top height was related to both climate and soil variables, supporting the background knowledge about this species, which indicates that its productivity is associated with moister conditions and soil water availability (Loguercio et al., 2018; Pastorino et al., 2015). Our analysis also showed that top height, thus productivity, decreases with summer temperature, which is directly related to evapotranspiration and water stress. Previous studies have indicated that *A. chilensis* growth declines as water loss by evapotranspiration predominates over precipitation inputs (Mundo et al., 2010). As found by tree-ring analysis, *A. chilensis* radial increment was negatively correlated with spring/summer temperatures (Landesmann et al., 2015; Roig and Villalba, 2008), a pattern also observed in other high-latitude forest regions such as North American Pacific Northwest (Case and Peterson, 2005). In the case of *A. chilensis*, stomatal control is the main physiological mechanism to avoid water stress (Gyenge et al., 2005) with consequent negative effects on tree growth (Marcotti et al., 2021; Pastorino et al., 2015). Thereby, top height increased with precipitation indicating that sites receiving higher water input would be favourable for *A. chilensis* growth. Overall, within the distribution range of the species, sites with greater water retention (as indicated by sand content –negative effect– and MAOM) and soil fertility (given by MAOM) (Grigal and Vance, 2000) were associated with better conditions for *A. chilensis* growth. The fact that the positive effect of precipitation may decrease with sand content suggests that even if rainfall was not limiting for growth, water may be lost by deep percolation before being used by trees (Tu et al., 2021). Indeed, dominant trees were taller in sites with greater content of soil organic matter associated to clay (MAOM) –a variable highly related with soil organic matter content (Pearson correlation = 0.91; Table A1). Soil organic matter is related to soil fertility and water retention (Wander, 2004).

Soil pH also appeared as a relatively important variable related with *A. chilensis* top height indicating that the height of *A. chilensis* dominant trees decreased towards soil acidity. The range of soil pH that we found (from 5.3 to 7.2) covered that usually observed in *A. chilensis* forests (Buamscha et al., 1998; La Manna, 2005; Mazzarino and Gobbi, 2005). Near-neutral pH soils are expected to be more productive than acid soils because the availability of nutrients for plant growth is reduced by soil acidity (Hong et al., 2018). Furthermore, *A. chilensis* produces alkaline leaf-litter (Mazzarino and Gobbi, 2005), thus forests that are more productive (more leaf-litter) may tend to increase soil pH. Importantly, soil nitrogen content, one of the most important nutrients related with plant growth and frequently the most-limiting nutrient in temperate forests (McLauchlan et al., 2017), was not related with *A. chilensis* top height. *A. chilensis* uses this nutrient efficiently and has a high capacity to conserve it irrespective of site characteristics (Buamscha et al., 1998), which may explain its low relation with *A. chilensis* top height.

Age indicates the elapsed time since tree establishment so that estimates of its effect are required in models evaluating temporal trends of stand structural characteristics. To address the inherently nonlinear age-height relationship (Hall and Bailey, 2001) we applied a log-transformation on age, finding that the observed pattern was well described (Figure A1). The best-ranked model indicated that the height of a dominant tree increases by about 5 m when age is doubled (e.g., from 45 to 90 yr., from 90 to 180 yr.). This model predicted an increment close to 11 m throughout the range of sampling age (from ≈45 yr. to ≈250 yr.) (Fig. 2a), resulting in a mean annual increment (MAI) of ≈0.06 m. Evaluating age classes similar to the one analysed in our study, Dezzotti and Sancholuz (1991) reported a range of slopes (from 0.02 m $yr.^{-1}$ to 0.8 m $yr.^{-1}$) that includes the MAI derived from our best-ranked model. These authors also indicated that slopes decreased with class age (steeper slopes on younger stands). Our sampling gathered two groups of ages, which ranged from ≈45 to ≈100 yr. and from ≈150 to ≈250 yr. (Fig. 2a). The sampling distribution is reflecting an age structure shaped by the disturbance regime: post-fire stands (younger group) and remnant stands –unaffected by fire– (older group) serving as seed sources for the former (Landesmann et al., 2015). When the best-ranked model is derivative at 70 yr. and 200 yr., (ages representing both age

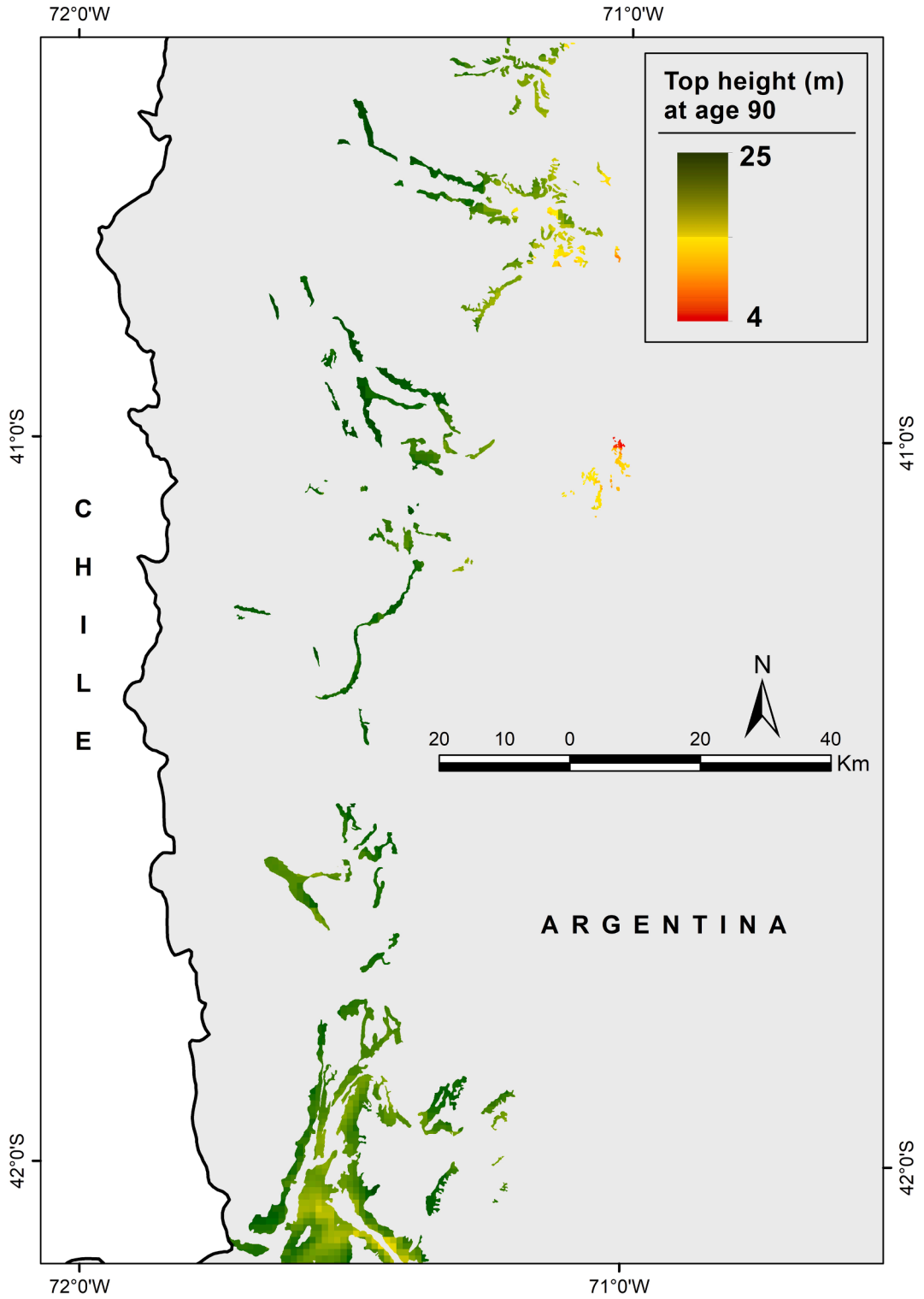

Fig. 4. Prediction map of *A. chilensis* top height at age 90 over the sampling area (darker green indicates better sites). Top height was predicted at the plot level running on each cell the simplest of the best-ranked climate/topography models, which only includes *age* (it was standardized at 90 years) and *summer temperature* as fixed predictors (Table 2).

groups) slopes decreases from ≈0.1 m yr.$^{-1}$ to ≈0.03 m yr.$^{-1}$, respectively (Fig. A.2 Appendices). Nevertheless. it would be worth to note that we did not develop temporal series, which could be considered as a limitation from a methodological perspective (Burkart and Tomé, 2012). In addition, the range of top heights predicted by the best-ranked climate-topography models at age 90 (among-plot variation around the intercept) covers that informed in other works at similar ages (Caselli, 2020; Goya et al., 2004; Loguercio et al., 2018). Because predictors were centered, the estimate for the intercept (≈17 m) indicates top height at the base age under average environmental conditions.

Developing regional site quality maps requires productivity models based on geographic information layers available at that scale. The increasing availability of remote sensed data makes satellite-based environmental information accessible. Climatic and topographic layers

Table A1
Pairwise Pearson's correlation between sampling environmental variables (Table 1). *expN* = northing; *expE* = easthing; *elev* = elevation; *Pp* = annual precipitation; *Ts* = mean summer temperature; *maom* = mineral-associated organic matter; *pom* = particulate organic matter; *som* = soil organic matter; *pmr* = POM:MAOM ratio; *P* = soil phosphorus content; *N* = soil nitrogen content; *ce* = soil electrical conductivity.

	Topography				Climate		Soil										
	expN	*expE*	*elev*	*slope*	*Pp*	*Ts*	*clay*	*silt*	*sand*	*maom*	*pom*	*som*	*pmr*	*P*	*N*	*pH*	*ce*
expN	1	0.16	0.16	0.1	0.24	0.11	−0.28	0.13	0.07	−0.27	−0.25	−0.31	0.06	−0.09	−0.15	−0.07	−0.12
expE	0.16	1	0.42	−0.16	−0.22	0.31	−0.24	−0.03	0.26	0.03	−0.25	−0.12	−0.26	0.07	−0.29	−0.1	−0.06
elev	0.16	0.42	1	−0.41	−0.11	−0.11	0.03	−0.19	0.16	−0.31	−0.32	−0.36	0.08	0.03	−0.58	−0.09	0.22
slope	0.1	−0.16	−0.41	1	0.02	0.2	0.08	−0.24	0.2	0.02	0	0.02	−0.19	−0.04	0.19	0.42	−0.16
Pp	0.24	−0.22	−0.11	0.02	1	−0.56	−0.21	0.29	−0.11	−0.36	−0.17	−0.29	0.2	0.09	0.11	−0.33	0.17
Ts	0.11	0.31	−0.11	0.2	−0.56	1	−0.16	−0.25	0.36	0.05	−0.07	−0.03	−0.28	0.11	−0.09	0.19	−0.34
clay	−0.28	−0.24	0.03	0.08	−0.21	−0.16	1	−0.51	−0.43	0.31	0.08	0.22	−0.23	0.03	−0.02	−0.06	0.24
silt	0.13	−0.03	−0.19	−0.24	0.29	−0.25	−0.51	1	−0.55	−0.23	−0.17	−0.22	0.1	−0.13	0.24	−0.17	−0.05
sand	0.07	0.26	0.16	0.2	−0.11	0.36	−0.43	−0.55	1	−0.05	0.11	0.03	0.14	0.07	−0.23	0.26	−0.18
maom	−0.27	0.03	−0.31	0.02	−0.36	0.05	0.31	−0.23	−0.05	1	0.63	0.91	−0.32	0.28	0.43	0.13	0.37
pom	−0.25	−0.25	−0.32	0	−0.17	−0.07	0.08	−0.17	0.11	0.63	1	0.9	0.44	0.32	0.44	0.2	0.21
som	−0.31	−0.12	−0.36	0.02	−0.29	−0.03	0.22	−0.22	0.03	0.91	0.9	1	0.05	0.29	0.48	0.18	0.3
pmr	0.06	−0.26	0.08	−0.19	0.2	−0.28	−0.23	0.1	0.14	−0.32	0.44	0.05	1	0.03	0.01	−0.05	−0.08
P	−0.09	0.07	0.03	−0.04	0.09	0.11	0.03	−0.13	0.07	0.28	0.32	0.29	0.03	1	0.31	0.2	0.59
N	−0.15	−0.29	−0.58	0.19	0.11	−0.09	−0.02	0.24	−0.23	0.43	0.44	0.48	0.01	0.31	1	−0.01	0.39
pH	−0.07	−0.1	−0.09	0.42	−0.33	0.19	−0.06	−0.17	0.26	0.13	0.2	0.18	−0.05	0.2	−0.01	1	−0.09
ce	−0.12	−0.06	0.22	−0.16	0.17	−0.34	0.24	−0.05	−0.18	0.37	0.21	0.3	−0.08	0.59	0.39	−0.09	1

can be easily obtained from global and regional data sources (e.g., (ASTER GDEM Validation Team, 2011; Bianchi et al., 2016; Farr et al., 2007; Fick and Hijmans, 2017; Hijmans et al., 2005), and global maps of soil properties have been generated recently (Hengl et al., 2017; Poggio et al., 2021). Although homogeneity in stand conditions is often assumed to simplify forest productivity modeling (Schlatter and Gerding, 2014), soil heterogeneity introduces spatial variability at finer-scales (Skovsgaard and Vanclay, 2013). In particular, the area of natural distribution of *A. chilensis* is characterized by a high edaphic heterogeneity (La Manna, 2005). On the other hand, unlike climate and topography variables, soil properties are laborious to measure in the field and require high-level technical expertise (Wander, 2004). Our data suggest that soil properties are as important as climatic variables in explaining top height (Table 2) although the loss of predictive capacity is not substantial if they are not included in the model (Table 4). Therefore, assuming that top height is a good indicator of *A. chilensis* productivity, simple climate models may serve as a rough guide to classify zones according to site quality (e.g., using only temperature as showed in Fig. 4). When required, the coarse regional classification could be improved at the operational scale by combining available soil maps with field-measured data (organic matter, pH, texture). This hierarchy between climate and soil matches that suggested in the literature for site classification factors (Schlatter and Gerding, 2014) as the basis of forest planning (from control-cut by area or volume scheduling to the setting of new areas for plantation). Considering the expected fluctuations in the climate of the Patagonian region in the next decades (Penalba and Rivera, 2016), and that *A. chilensis* is suggested to be affected by these climactic fluctuations (Marcotti, 2019), our model might be used to foresee climate change effects on forest productivity (Sharma et al., 2015). Importantly, our study did not include aspects of genetic variability, which affects spatial variability in the size of trees and may confound site effects (Skovsgaard and Vanclay, 2013). The area where the lowest top height are predicted (Fig. 4) matches the eastern marginal populations of *A. chilensis* although our model do not generate the longitudinal pattern of genetic variability described for this species (see Fig. 2 in Pastorino et al. 2015). This could be suggesting that a considerable part of the genetic variability of this species was included within the error components of our statistical model.

In short, this study provides a set of environmental indicators of productivity useful for mapping *A. chilensis* site quality at different levels of detail (regional, forest, stand, management unit) depending on the specific forestry objective (Skovsgaard and Vanclay, 2013). Considering the current legal framework of Argentina promotes native species plantations, it contributes to design new *A. chilensis* plantations in northern Patagonia and, hence, to address future timber and ecosystem services demands. Moreover, the model has potential usefulness beyond forestry. From a methodological point of view, by applying a multi-model framework, our work shows an approach that, contrary to its increasingly adoption in ecology, is not commonly used in modeling forest site productivity (Aertsen et al., 2010).

5. Conclusions

Our multi-modeling approach, which accounts for the effects of environmental factors on *A. chilensis* top height (a vegetation-based indicator of productivity), is intended as a first step toward regional cartography of site quality in northern Patagonia. Top height of *A. chilensis* was explained by both climate and soil properties; dominant trees were taller in cooler and wetter sites, and where soil retains more water, stores more carbon, and has lower acidity. When including only climate variables, the explained variance was reduced although the loss of predictive capability was not substantial. We suggest that site quality for *A. chilensis* can be roughly classified from a few climatic (for example by using only summer temperature) variables available in satellite-based geospatial information. Then, if required, the initial classification could be improved by adding soil information. Being the first regional

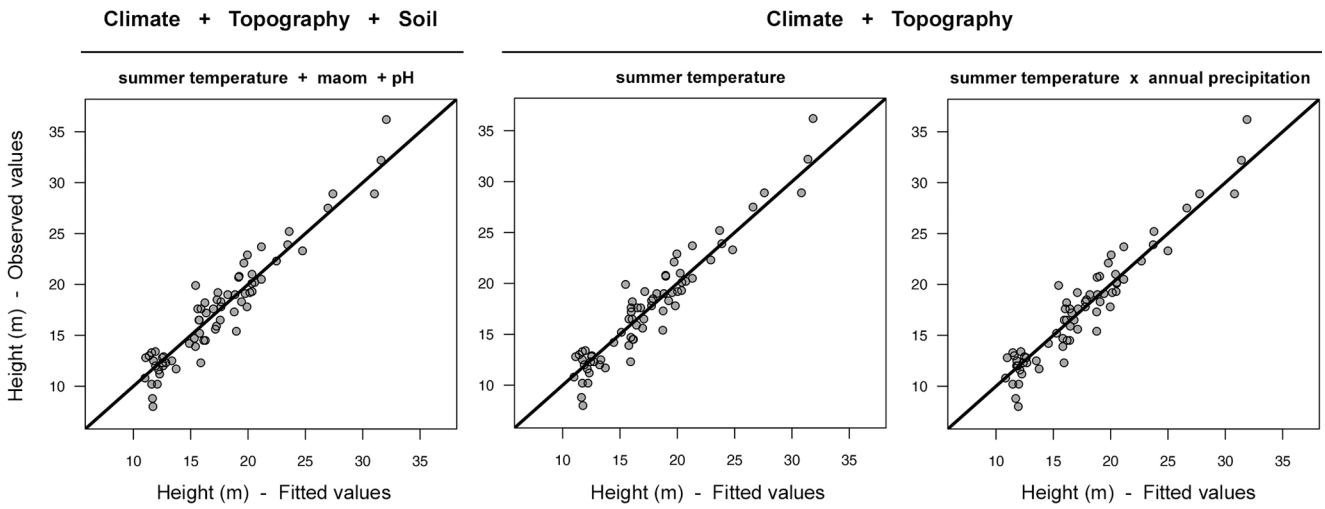

Fig. A1. Graphical assessment of model fit for top height of *A.chilensis*. The panel shows the observed height in dominant trees versis fitted values for three different models. The first plot (left-side) corresponds to the best-ranked model (overall fit, that is, considering soil, climate conditions, and topography as predictors). The second (centre) and third (right-side) plots correspond to the best models obtained when soil was excluded from the models (these models ranked 24th and 76th overall, respectively; Table 2). All models included the *age* of *A. chilensis* dominant trees as predictor.

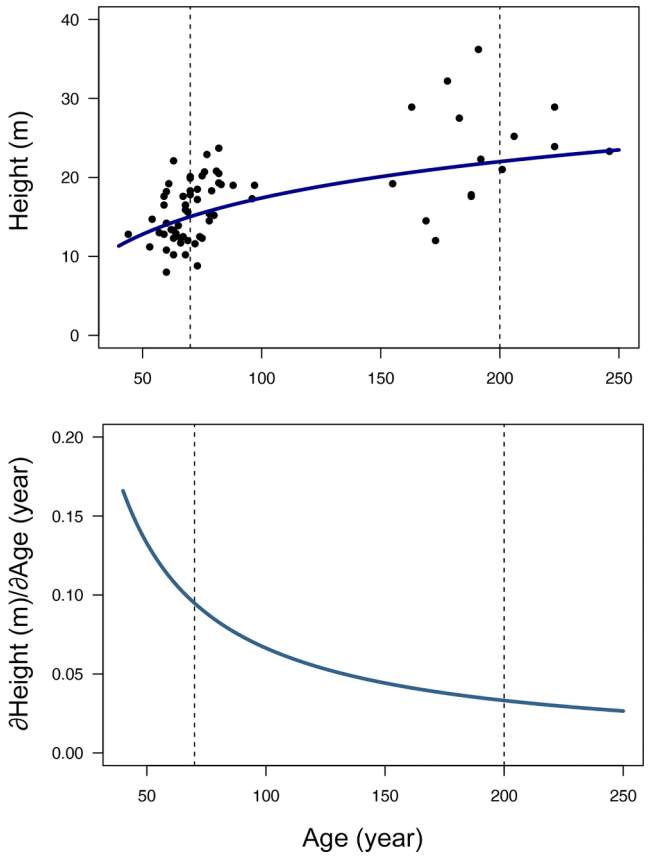

Fig. A2. *A. chilensis* growth rate inferred from the best-ranked model (Table 3). Solid line in the upper-plot shows *A. chilensis* top height predicted from the best-ranked model along age when the remaining predictors (summer temperature, MAOM,and soil pH) are keep at the mean value. Points show the observed data. Solid line in the bottom-plot shows the growth rate obtained as the derivative of top height respect to age. Vertical dotted lines at 70 and 200 on *x*-axis highlight ages representing the two age classes sampled.

statistical model predicting productivity of *A. chilensis*, it becomes a valuable tool for the sustainable management of this native species. Interestingly, our model has potential usefulness beyond forestry, for instance, to evaluate climate change effects on ecosystem services related to forest productivity.

Author contributions

FJO, MGG, CC and LAG laid out the manuscript, LAG, JG and TK designed the sampling, CC, JPL, and JL carried out the field sampling, FJO and CC performed the data analysis, FJO led the writing and all co-authors contributed with ideas and edited the text.

Declaration of Competing Interest

The authors declare that they have no known competing financial interests or personal relationships that could have appeared to influence the work reported in this paper.

Data availability

Data will be made available on request.

Acknowledgments

This work was supported by grants from FONCYT (PICT 2019-00393; PICT 2016-0305) and UNRN (PI 40-B-892; PI 40-13-635; PI 40-B-510). We thank Ana Morant and José L. Langlois for field assistant.

Appendix

Appendices - equations

Linear mixed-effects model

$$h_{ij} \sim N\left(\mu_i; \sigma^2\right)_{indep} \tag{A1}$$

$$\mu_i = \beta_{0j} + \beta_1 \times age_i$$

$$\beta_{0j} \sim N\left(\mu_{\beta_{0j}}; \sigma^2_{\beta_0}\right)$$

$$\mu_{\beta_{0j}} = \alpha_0 + \alpha_1 \times Pp_j + \alpha_2 \times Ts_j + \alpha_3 \times elev_j + \alpha_4 \times slope_j + \alpha_5 \times expN_j + \alpha_6 \times maom_j + \alpha_7 \times pmr_j + \alpha_8 \times N_j + \alpha_8 \times P_j + \alpha_9 \times sand_j + \alpha_{10} \times pH_j + \alpha_{11} \times ec_j + \alpha_{12} \times Pp_j \times Ts_j + \alpha_{13} \times Pp_j \times expN_j + \alpha_{14} \times Ts_j \times maom_j + \alpha_{15} \times Pp_j \times maom_j + \alpha_{16} Pp_j \times sand_j$$

where h_{ij} is the height of the *i*th dominant tree in the *j*th plot. Variance inflation factor (VIF) values for predictors: *age* = 2.7; *Pp* = 9.8; *Ts* = 9.6; *maom* = 8.2; *pmr* = 2.4; *N* = 3.7; *P* = 4.2; *sand* = 3.2; *pH* = 3.2; *ec* = 6.7; *Ts*:*maom* = 5.7; *Pp*:*maom* = 8.8; *Pp*:*sand* = 4.3.

Metrics of prediction capability

$$mae = \frac{1}{NT}\sum_{j=1}^{p}\sum_{i=1}^{q}\left|h_{ij} - \widehat{h}_{ij}\right| \tag{A2}$$

$$mape = \frac{1}{NT}\sum_{j=1}^{p}\sum_{i=1}^{q}\left|h_{ij} - \widehat{h}_{ij}\right| \Big/ h_{ij} \times 100 \tag{A3}$$

where h_{ij} and $\widehat{h}_{ij}$ are the heights observed and predicted for the *i*th dominant tree of the *j*th plot, respectively; *p* is the number of plots in a testing subset; *q* is the number of dominant trees in the *j*th plot; *NT* is the total number of dominant tress in all plots in the testing subset being evaluated.

References

Aertsen, W., Kint, V., van Orshoven, J., Özkan, K., Muys, B., 2010. Comparison and ranking of different modelling techniques for prediction of site index in Mediterranean mountain forests. Ecol. Modell. 221, 1119–1130. https://doi.org/10.1016/j.ecolmodel.2010.01.007.

Aparicio, A.G., Pastorino, M.J., 2020. Patagonian Cypress (Austrocedrus chilensis): The Cedarwood of the Emblematic Architecture of North Patagonia. In: Pastorino, M.J., Paula, M. (Eds.), Low Intensity Breeding of Native Forest Trees in Argentina. Springer Nature, pp. 149–174. https://doi.org/10.1007/978-3-030-56462-9.

Assmann, E., 1970. The Principles of Forest Yield Study. Pergamon Press.

ASTER GDEM Validation Team, 2011. ASTER Global DEM Validation Summary Report, ASTER GDEM Validation Team [WWW Document]. METI, NASA USGS Coop. with NGA other Collab.

Barton, K., 2020. _MuMIn: Multi-Model Inference_. R package version 1 (46).

Bianchi, E., Villalba, R., Viale, M., Couvreux, F., Marticorena, R., 2016. New precipitation and temperature grids for northern Patagonia: advances in relation to global climate grids. J. Meteorol. Res. 30, 38–52. https://doi.org/10.1007/s13351-015-5058-y.

Bontemps, J.D., Bouriaud, O., 2014. Predictive approaches to forest site productivity: recent trends, challenges and future perspectives. Forestry 87, 109–128. https://doi.org/10.1093/forestry/cpt034.

Bremner, J.M., 1960. Determination of nitrogen in soil by the Kjeldahl method. J. Agric. Sci. 55, 11–33. https://doi.org/10.1017/S0021859600021572.

Buamscha, G., Gobbi, M., Mazzarino, M.J., Laos, F., 1998. Indicators of Nitrogen economy in Austrocedrus chilensis forest along a moisture gradient. For. Ecol. Manage. 112, 253–261.

Burkart, A.E., Tomé, M., 2012. Evaluating site quality. Modelling Forest Trees and Stands. Springer 131–174.

Burnham, K.P., Anderson, D.R., Huyvaert, K.P., 2011. AIC model selection and multimodel inference in behavioral ecology: some background, observations, and comparisons. Behav. Ecol. Sociobiol. 65, 23–35. https://doi.org/10.1007/s00265-010-1029-6.

Cambardella, C.A., Elliott, E.T., 1992. Particulate soil organic-matter changes across a grassland cultivation sequence. Soil Sci. Soc. Am. J. 56, 777–783. https://doi.org/10.2136/sssaj1992.03615995005600030017x.

Case, M.J., Peterson, D.L., 2005. Fine-scale variability in growth-climate relationships of Douglas-fir, North Cascade Range. Washington. Can. J. For. Res. 35, 2743–2755.

Caselli, M., 2020. Crecimiento de Austrocedrus chilensis y Nothofagus dombeyi en bosques mixtos y condiciones ambientales para el desarrollo de sus renovales: contribuciones al manejo de rodales afectados por el mal del ciprés. Universidad Nacional de La Plata, Tesis Doctoral.

Castor, C., Cuevas, J.G., Kalin Arroyo, M.T., Rafii, Z., Dodd, R., Peñaloza, A., 1996. Austrocedrus chilensis (D. Don) Pic.-Ser. et Bizz. (Cupressaceae) from Chile and Argentina: monoecious or dioecious? Rev. Chil. Hist. Nat. 69, 89–95.

Cinar, O., Umbanhowar, J., Hoeksema, J.D., Viechtbauer, W., 2021. Using information-theoretic approaches for model selection in meta-analysis. Res. Synth. Methods 12, 537–556. https://doi.org/10.1002/jrsm.1489.

Cordon, V., Forquera, J., Gastiazoro, J., 1993. Estudio microclimático del área cordillerana del sudoeste de la provincia de Río Negro. Cartas de Precipitación, Cinco Saltos.

ORNL DAAC, 2011. MODIS Collection 5 Land Products Global Subsetting and Visualization Tool. ORNL DAAC, Oak Ridge, Tennessee, USA.

Davis, A.S., Jacobs, D.F., Dumroese, R.K., 2012. Challenging a paradigm: toward integrating indigenous species into tropical plantation forestry 293–308. https://doi.org/10.1007/978-94-007-5326-6_15.

Dezzotti, A., Sancholuz, L., 1991. Los bosques de Austrocedrus chilensis en Argentina: ubicación, estructura y crecimiento. Bosque 12, 43–52. https://doi.org/10.4206/bosque.1991.v12n2-04.

Donoso, J.P., Soto, D.P., 2010. Plantaciones con especies nativas en el centro-sur de Chile: experiencias, desafios y oportunidades. Revista Bosque Nativo 47.

Duncan, R.P., 1989. An evaluation of errors in tree age estimates basedon increment cores of Kahikatea (Dacrycarpus dacrydioides). New Zeal. Nat. Sci. J. 16, 31–37.

Eastman, J.R., 2009. IDRISI taiga, guide to GIS and remote processing. Clark University, Worcester, Clark Labs for Cartographic Technology and Geographic Analysis.

FAO and UNEP, 2020. The State of the World's Forests, In brief. Forests, biodiversity and people. FAO, Rome. https://doi.org/10.1515/9783035608632-002.

Farr, T.G., Rosen, P.A., Caro, E., Crippen, R., Duren, R., Hensley, S., Kobrick, M., Paller, M., Rodriguez, E., Roth, L., Seal, D., Shaffer, S., Shimada, J., Umland, J., Werner, M., Oskin, M., Burbank, D., Alsdorf, D., 2007. The shuttle radar topography mission. Rev. Geophys. 45, RG2004. https://doi.org/10.1007/3-540-44818-7_11.

Fick, S.E., Hijmans, R.J., 2017. WorldClim 2: new 1-km spatial resolution climate surfaces for global land areas. Int. J. Climatol. 37, 4302–4315.

Goldenberg, M.G., Gowda, J.H., Casas, C., Garibaldi, L.A., 2018. Efecto de la tasa de descuento sobre la priorización de alternativas de manejo del matorral Norpatagónico argentino. Bosque 39, 217–226. https://doi.org/10.4067/S0717-92002018000200217.

Gowda, J.H., Kitzberger, T., Edwards, P., 2010. Comunidades vegetales y ecosistemas terrestres: segundo informe de avance. Argentina.

Goya, J.F., Ferrando, J.J., Yapura, P.F., 2004. Aspectos silviculturales de los bosques de Austrocedrus chilensis de la región de El Bolsón, Río Negro. Ecol. y manejo los bosques Argentina 1–18.

Grigal, D.F., Vance, E.D., 2000. Influence of soil organic matter on forest productivity. New Zeal. J. For. Sci. 30, 169–205.

Gyenge, J., Fernández, M., Dalla Salda, G., Schlichter, T., 2005. Leaf and whole-plant water relations of the Patagonian conifer Austrocedrus chilensis (D. Don) Pic. Ser. et Bizzarri: implications on its drought resistance capacity. Ann. For. Sci. 62, 297–302. https://doi.org/10.1051/forest:2005024.

Hall, D.B., Bailey, R.L., 2001. Modeling and prediction of forest growth variables based on multilevel nonlinear mixed models. For. Sci. 47 (3), 311–321. https://doi.org/10.1093/forestscience/47.3.311.

Hengl, T., De Jesus, J.M., Heuvelink, G.B.M., Gonzalez, M.R., Kilibarda, M., Blagotić, A., Shangguan, W., Wright, M.N., Geng, X., Bauer-Marschallinger, B., Guevara, M.A., Vargas, R., MacMillan, R.A., Batjes, N.H., Leenaars, J.G.B., Ribeiro, E., Wheeler, I., Mantel, S., Kempen, B., 2017. SoilGrids250m: global gridded soil information based on machine learning. PLoS ONE. https://doi.org/10.1371/journal.pone.0169748.

Hijmans, R.J., Cameron, S.E., Parra, J.L., Jones, P.G., Jarvis, A., 2005. Very high resolution interpolated climate surfaces for global land areas. Int. J. Climatol. 25, 1965–1978.

Hong, S., Piao, S., Chen, A., Liu, Y., Liu, L., Peng, S., Sardans, J., Sun, Y., Peñuelas, J., Zeng, H., 2018. Afforestation neutralizes soil pH. Nat. Commun. 9, 520. https://doi.org/10.1038/s41467-018-02970-1.

Kottek, M., Grieser, J., Beck, C., Rudolf, B., Rubel, F., 2006. World map of the Köppen-Geiger climate classification updated. Meteorol. Zeitschrift 15, 259–263. https://doi.org/10.1127/0941-2948/2006/0130.

La Manna, L., 2005. Caracterización de los suelos bajo bosque de Austrocedrus chilensis a través de un gradiente climático y topográfico en Chubut, Argentina. Bosque 26, 137–153. https://doi.org/10.4067/s0717-92002005000200017.

Ladio, A., 2005. La potencialidad de los bosques de cipres, como proveedores de recursos forestales no maderables. Patagon. For. 2, 14–17.

Landesmann, J.B., Gowda, J.H., Garibaldi, L.A., Kitzberger, T., 2015. Survival, growth and vulnerability to drought in fire refuges: implications for the persistence of a fire-sensitive conifer in northern Patagonia. Oecologia 179, 1111–1122. https://doi.org/10.1007/s00442-015-3431-2.

Letourneau, F., Schlichter, T., Andenmatten, E., 2005. Manejo Silvícola de Renovales de Ciprés de la Cordillera. idia XXI Rev. Inf. sobre Investig. y Desarro. Agropecu. 8, 80–83.

Loguercio, G.A., Claverie, H., Rey, M.A., 2005. Posibilidades de Manejo Forestal de los Bosques de Ciprés de la Cordillera. idia XXI Rev. Inf. sobre Investig. y Desarro. Agropecu. 8, 84–88.

Loguercio, G.A., Urretavizcaya, M.F., Caselli, M., Defossé, G.E., 2018. Propuestas silviculturales para el manejo de bosques de bosques de Austrocedrus chilensis sanos y afectados por el mal del ciprés de Argentina, in: Donoso, P.J., Promis, Á., Soto, D.P. (Eds.), Silvicultura En Bosques Nativos. Experiencias En Silvicultura y Restauración En Chile, Argentina y El Oeste de Estados Unidos. Imprenta America, Valdivia, pp. 117–131.

Marcotti, E., 2019. Response of the growth of Austrocedrus Chilensis to the climatic variations in the north of the Patagonia: implications because of the climate changes. Universidad Nacional de Córdoba.

Marcotti, E., Amoroso, M.M., Rodríguez-Catón, M., Vega, L., Srur, A.M., Villalba, R., 2021. Growth resilience of Austrocedrus chilensis to drought along a precipitation gradient in Patagonia. Argentina. For. Ecol. Manage. 496, 119388 https://doi.org/10.1016/j.foreco.2021.119388.

Matteucci, S.D., 2012. Ecorregión Bosques Patagónicos. In: Morello, J., Matteucci, S.D., Rodriguez, A.M.S. (Eds.), Ecorregiones Y Complejos Ecosistémicos Argentinos. Orientación Gráfica Editora, Buenos Aires, pp. 489–547.

Mazzarino, M.J., Bertiller, M., Schilchter, T., Gobbi, M.E., 1998. Nutrient cycling in Patagonia ecosystems. Ecol. Austral 8, 167–181.

Mazzarino, M., Gobbi, M., 2005. Indicadores de Circulación de Nutrientes en Bosques Andino-Patagónicos. Idia 15–18.

McLauchlan, K.K., Gerhart, L.M., Battles, J.J., Craine, J.M., Elmore, A.J., Higuera, P.E., Mack, M.C., McNeil, B.E., Nelson, D.M., Pederson, N., Perakis, S.S., 2017. Centennial-scale reductions in nitrogen availability in temperate forests of the United States. Sci. Rep. 7, 7856. https://doi.org/10.1038/s41598-017-08170-z.

Mirsky, S.B., Lanyon, L.E., Needelman, B.A., 2008. Mechanical grinding for particulate organic-matter analysis. Commun. Soil Sci. Plant Anal. 39, 1147–1153. https://doi.org/10.1080/00103620801925844.

Mundo, I.A., El Mujtar, V.A., Perdomo, M.H., Gallo, L.A., Villalba, R., Barrera, M.D., 2010. Austrocedrus chilensis growth decline in relation to drought events in northern Patagonia, Argentina. Trees 24, 561–570. https://doi.org/10.1007/s00468-010-0427-8.

Nakagawa, S., Schielzeth, H., 2013. A general and simple method for obtaining R 2 from generalized linear mixed-effects models. Methods Ecol. Evol. 2, 133–142. https://doi.org/10.1111/j.2041-210x.2012.00261.x.

O'Hara, K.L., 2016. What is close-to-nature silviculture in a changing world? Forestry 89, 1–6. https://doi.org/10.1093/forestry/cpv043.

Oddi, F.J., Goldenberg, M.G., Nacif, M., Heinemann, K., Garibaldi, L.A., 2021. Supervivencia y crecimiento de plantines de ciprés de la cordillera durante siete años en dos sitios contrastantes de Patagonia norte. Ecol. Austral 31, 204–215.

Olsen, L.R., 2021. _cvms: Cross-Validation for Model Selection_. R package version 1 (3), 4.

Olsen, L.R., Zachariae, H.B., 2021. cvms: Cross-Validation for Model Selection.

Pansu, M., Gautheyrou, J., 2006. Particle Size Analysis. In: Pansu, M., Gautheyrou, J. (Eds.), Handbook of Soil Analysis: Mineralogical, Organic and Inorganic Methods. Springer, Berlin Heidelberg, pp. 15–63. https://doi.org/10.1007/978-3-540-31211-6_2.

Paruelo, J.M., Beltran, A., Jobbagy, E., Sala, O.E., Golluscio, R.A., 1998. The climate of Patagonia: General patterns and controls on biotic processes. Ecol. Austral 8, 85–101.

Pastorino, M.J., Fariña, M., Bran, D., Gallo, L., 2006. Extremos geográficos de la distribución natural de Austrocedrus chilensis (Cupressaceae). Boletín la Soc. Argentina Botánica 41, 307–311.

Pastorino, M.J., Aparicio, A.G., Azpilicueta, M.M., 2015. Regiones de Procedencia del Ciprés de la Cordillera y bases conceptuales para el manejo de sus recursos genéticos en Argentina. Ediciones INTA, Buenos Aires.

Penalba, O.C., Rivera, J.A., 2016. Regional aspects of future precipitation and meteorological drought characteristics over Southern South America projected by a CMIP5 multi-model ensemble. Int. J. Climatol. 36, 974–986. https://doi.org/10.1002/joc.4398.

Pinheiro J, Bates D, DebRoy S, Sarkar D, R.C.T., 2020. _nlme: Linear and Nonlinear Mixed Effects Models_.

Poggio, L., De Sousa, L.M., Batjes, N.H., Heuvelink, G.B.M., Kempen, B., Ribeiro, E., Rossiter, D., 2021. SoilGrids 2.0: Producing soil information for the globe with quantified spatial uncertainty. Soil 7, 217–240. https://doi.org/10.5194/soil-7-217-2021.

R Core Team, 2020. R: A Language and Environment for Statistical Computing.

Roig, F.A., Villalba, R., 2008. Understanding Climate from Patagonian Tree Rings. In: Rabassa, J. (Ed.), Developments in Quaternary Science. Elsevier, pp. 411–435. https://doi.org/10.1016/S1571-0866(07)10021-X.

Promis, A., 2020. Plantaciones nativas o exóticas: Reflexiones sobre los impactos ambientales en Chile. Ecol. Austral 30, 191–198. https://doi.org/10.25260/EA.20.30.2.0.1064.

Schlatter, J., Gerding, V., 2014. Sitio forestal. In: Donoso, C., González, M.E., Lara, A. (Eds.), Ecología Forestal. Bases Para El Manejo Sustentable y Conservación de Los Bosques Nativos de Chile, Ediciones UACh, Valdivia, pp. 309–319.

Serra, M.T., Cruz, G.M., Promis, A., 2015. Antecedentes generales de ciprés de la cordillera (Austrocedrus chilensis). In: Cruz, G.M. (Ed.), Ciprés de La Cordillera (Austrocedrus Chilensis (D. Don) Pic. Serm. et Bizarri). Antecedentes Ecológicos Para La Conservación de Las Comunidades En El Alto Cachapoal. Maval, pp. 37–129.

Sharma, M., Subedi, N., Ter-Mikaelian, M., Parton, J., 2015. Modeling climatic effects on stand Height/Site index of plantation-grown jack pine and black spruce trees. For. Sci. 61, 25–34. https://doi.org/10.5849/forsci.13-190.

Pro Silva, 2012. Pro Silva Principles. Pro Silva – Association of European Foresters Practicing Management which follows Natural Processes, Truttenhausen.

Skovsgaard, J.P., Vanclay, J.K., 2008. Forest site productivity: a review of the evolution of dendrometric concepts for even-aged stands. Forestry 81, 13–31. https://doi.org/10.1093/forestry/cpm041.

Skovsgaard, J.P., Vanclay, J.K., 2013. Forest site productivity: a review of spatial and temporal variability in natural site conditions. Forestry 86, 305–315. https://doi.org/10.1093/forestry/cpt010.

Tu, A., Xie, S., Mo, M., Song, Y., Li, Y., 2021. Water budget components estimation for a mature citrus orchard of southern China based on HYDRUS-1D model. Agric. Water Manag. 243, 106426 https://doi.org/10.1016/j.agwat.2020.106426.

Veblen, T.T., Burns, B.R., Kitzberger, T., Lara, A., Villalba, R., 1995. The Ecology of the conifers of Southern South America. In: Enright, N.J., Hills, R.S. (Eds.), Ecology of the Southern Conifers. Melbourne University Press, Carlton, pp. 120–155.

Veblen, T.T., Armesto, J.J., Burns, B.R., Kitzberger, T., Lara, A., Young, R., 2005. The coniferous forests of south america. In: Andersson, F.A. (Ed.), Ecosystems of the World, Coniferous Forests. Elsevier, Amsterdam, pp. 701–725.

Veblen, T.T., Lorenz, D.C., 1987. Post-fire development of Austrocedurs-Nothofagus forests in nothern Patagonia. Vegetatio 71, 113–126.

Villalba, R., Veblen, T.T., 1997. Regional patterns of tree population age structures in Northern Patagonia: climatic and disturbance influences. J. Ecol. 85, 113–124.

Wander, M., 2004. Soil Organic Matter Fractions and Their Relevance to Soil Function. In: Magdoff, F., Weil, R.R. (Eds.), Soil Organic Matter in Sustainable Agriculture. CRC Press, New York, pp. 67–102. https://doi.org/10.1201/9780203496374.ch3.

Weiskittel, A.R., Crookston, N.L., Radtke, P.J., 2011. Linking climate, gross primary productivity, and site index across forests of the western United States. Can. J. For. Res. 41, 1710–1721. https://doi.org/10.1139/x11-086.

Yang, Y., Huang, S., 2014. Suitability of five cross validation methods for performance evaluation of nonlinear mixed-effects forest models - A case study. Forestry 87, 654–662. https://doi.org/10.1093/forestry/cpu025.

Zuur, A.F., Ieno, E.N., Walker, N., Saveliev, A.A., Smith, G.M., 2009. Mixed effects models and extensions in ecology with R. Springer, New York.

QGIS Development Team. 2019. QGIS Geographic Information System. Open Source Geospatial Foundation Project. Available from http://qgis.osgeo.org.